Supporting Information

A New Ferroelastic Hybrid Material with a Large Spontaneous Strain: $(Me_3NOH)_2[ZnCl_4]$

Wei Yuan,[a] *Ying Zeng,*[a] *Ya-Yin Tan,*[b] *Jian-Hua Zhou,*[b] *Wei-Jian Xu,*[a,c,*] *Wei-Xiong Zhang*[a,*] *and Xiao-Ming Chen*[a]

[a] MOE Key Laboratory of Bioinorganic and Synthetic Chemistry, School of Chemistry, Sun Yat-Sen University, Guangzhou, 510275, P. R. China.

[b] Key Laboratory of Sensing Technology and Biomedical Instruments of Guangdong Province, School of Biomedical Engineering, Sun Yat-Sen University, Guangzhou 510275, China.

[c] Department of Chemistry & CICECO-Aveiro Institute of Materials, University of Aveiro, 3810-193 Aveiro, Portugal.

Experimental

Synthesis

Trimethylamine N-oxide hydrochloride was obtained by reaction of trimethylamine N-oxide dehydrate with 36.5% aqueous HCl. All the other chemicals were commercially available and were used without further purification.

Compound **1** was synthesized by mixing aqueous solutions of $ZnCl_2$, HCl (36.5%), and trimethylamine N-oxide hydrochloride in the ratio of 1:2:1. Block colourless single crystals were obtained by slow evaporation of solvent at room temperature after a few days. The bulk phase purity was confirmed by powder X-ray diffraction (Fig. S1). Elemental analysis, calcd (%) for 1 ($C_6H_{20}Cl_4N_2O_2Zn$, 359.46): C, 20.05; N, 7.79; H, 5.61. Found, C, 20.26; N, 7.73; H, 6.17."

Single-crystal X-ray crystallography

The *in-situ* variable-temperature single-crystal X-ray diffraction intensities were collected on a RigakuXtaLAB P300DS single-crystal diffractometer with graphite monochromated Cu-Kα radiation (λ = 1.54178 Å). The CrystalClear software package (Rigaku) was used for data collection, cell refinement, and data reduction. Absorption corrections were applied by using multi-scan program REQAB (Jacobson, 1998). The structures were solved by direct methods and refined using full-matrix least-squares methods with the SHELX program package and Olex2 program.[1] Non-hydrogen atoms were refined anisotropically and the positions of the hydrogen atoms were generated geometrically. The crystal data and structure refinement results at different temperatures for **1** are listed in Table S1. Selected bond distances and bond angles are listed in Table S2 and S3.

Thermogravimetric analyses

Thermogravimetric analyses (TGA) were carried out on a TA Q50 system with a heating rate of 5 K min^{-1} under a nitrogen atmosphere.

DSC measurements

Differential scanning calorimetry (DSC) was carried out on a TA DSC Q2000 instrument under a nitrogen atmosphere in aluminum crucibles with heating and cooling rates of 10 K/min from 293 K to 393 K.

Dielectric measurements

The dielectric measurements were carried on a TH2828A impedance analyzer for **1** from 500 Hz to 1 MHz, with an amplitude of 1.0 V, and a temperature sweeping rate of approximately 5 K/min for **1** in a Mercury iTC cryogenic environment controller of Oxford Instrument. The pressed-powder pellets were deposited with silver conducting glue used as electrodes.

Variable-temperature powder X-ray diffraction (PXRD)

Variable temperature PXRD patterns (Cu Kα, λ = 1.54178 Å) were collected on Bruker Advance D8 DA VANCI diffractometer for **1** in the temperature range of 303–383 K.

Variable-temperature polarization microscopy

Variable-temperature polarization microscopy observations were carried out with a polarizing microscope Leica DM2500 P equipped with a Linkam cooling/heating stage THMSE 600. The temperature was stabilized with an accuracy of ±0.1 K.

Elemental analysis

Elemental (C, H, and N) analyses were performed on a Perkin-Elmer Vario EL elemental analyzer with as-synthesized samples.

Deduction of domain orientation

During the phase transition from *Pnma* (**HTP**) to $P2_1/n11$ (**RTP**), a symmetry breaking occurs from 8 (E, i, $3C_2$, 3σ) to 4 (E, i, C_2, σ_h) symmetry elements, classifying **1** to be an *mmm*F2/*m* ferroelastic species with two possible orientation states in the ferroelastic phase, according to Aizu.[2] The spontaneous strain within these two states are expressed as

$$\varepsilon_{ij}^{(1)} = \begin{bmatrix} \varepsilon_{11} & 0 & 0 \\ 0 & \varepsilon_{22} & \varepsilon_{23} \\ 0 & \varepsilon_{23} & \varepsilon_{33} \end{bmatrix},\ \varepsilon_{ij}^{(2)} = \begin{bmatrix} \varepsilon_{11} & 0 & 0 \\ 0 & \varepsilon_{22} & -\varepsilon_{23} \\ 0 & -\varepsilon_{23} & \varepsilon_{33} \end{bmatrix}$$

The modified spontaneous strains proposed by Aizu[3] are then

$$\varepsilon_{sij}^{(i)} = \varepsilon_{ij}^{(i)} - \frac{1}{q}\sum_{k=1}^{q} \varepsilon_{ij}^{(k)}\ \ (i = 1, 2, \dots, q)$$

In this case,

$$\varepsilon_{sij}^{(1)} = \begin{bmatrix} 0 & 0 & 0 \\ 0 & 0 & \varepsilon_{23} \\ 0 & \varepsilon_{23} & 0 \end{bmatrix}, \varepsilon_{sij}^{(2)} = \begin{bmatrix} 0 & 0 & 0 \\ 0 & 0 & -\varepsilon_{23} \\ 0 & -\varepsilon_{23} & 0 \end{bmatrix}$$

considering the compatibility condition of spontaneous strain[4]

$$[\varepsilon_{sij}^{(1)} - \varepsilon_{sij}^{(2)}]x_i x_j = 0$$

where x_i and x_j are components of unit vector on domain walls, we obtain $2\varepsilon_{23}yz = 0$, which gives the orientation of domain walls $y = 0$ and $z = 0$.

Table S1. Crystal data and structure refinement parameters for **1** at **RTP** and **HTP**.

Compound	**1**	
Formula	$(Me_3NOH)_2[ZnCl_4]$	
T (K)	293(2)	373(2)
Phases	RTP	HTP
Crystal system	Monoclinic	Orthorhombic
Space group	$P2_1/n11$	*Pnma*
a/Å	12.2339(2)	12.2052(6)
b/Å	8.5620(1)	8.7156(4)
c/Å	15.2029(3)	15.4497(7)
α/°	100.244(2)	90
V/Å^3	1567.07(5)	1643.5(2)
Z	4	4
D_c /g cm^{-3}	1.523	1.453
reflns coll.	3148	1548
unique reflns	2872	945
R_1 [$I > 2\sigma(I)$]	0.0393	0.1131
wR_2 [$I > 2\sigma(I)$]	0.1125	0.4149
R_1 [a] (all data)	0.0414	0.1243
wR_2 [b] (all data)	0.1162	0.4536
GOF	1.080	1.088
CCDC number	1915260	1915261

[a] $R_1 = \sum||F_o| - |F_c||/\sum|F_o|$, [b] $wR_2 = \{\sum w[(F_o)^2 - (F_c)^2]^2/\sum w[(F_o)^2]^2\}^{1/2}$

Table S2. Selected bond lengths (Å) for **1** at **RTP** and **HTP**.

RTP		**HTP**	
Zn1–Cl1	2.2472(7)	Zn1–Cl1$^{\#1}$	2.216(2)
Zn1–Cl2	2.2375(8)	Zn1–Cl1	2.216(2)
Zn1–Cl3	2.2999(7)	Zn1–Cl2	2.251(3)
Zn1–Cl4	2.2807(7)	Zn1–Cl3	2.243(3)
N1–O1	1.421(2)	N1–O1	1.426(9)
N1–C1	1.480(3)	N1–C1	1.474(9)
N1–C2	1.475(3)	N1–C2	1.497(9)
N1–C3	1.478(3)	N1–C3	1.456(9)
N2–O2	1.427(3)	N2–O2	1.426(9)
N2–C4	1.471(4)	N2–C4	1.470(9)
N2–C5	1.451(4)	N2–C5	1.463(9)
N2–C6	1.486(4)	N2–C6	1.482(9)

Symmetry codes: #1, (*x*, 1/2-*y*, *z*)

Table S3. Selected bond angles (°) for **1** at **RTP** and **HTP**.

RTP		**HTP**	
Cl1–Zn1–Cl2	111.88(4)	Cl1–Zn1–Cl1$^{\#1}$	108.1(2)
Cl1–Zn1–Cl3	107.46(3)	Cl1–Zn1–Cl2	109.5(2)
Cl1–Zn1–Cl4	109.47(3)	Cl1–Zn1–Cl3	109.1(2)
Cl2–Zn1–Cl3	110.73(3)	Cl2–Zn1–Cl3	111.4(2)
Cl2–Zn1–Cl4	109.83(3)	O1–N1–C1	103.0(12)
Cl3–Zn1–Cl4	107.33(3)	O1–N1–C2	106.6(12)
O1–N1–C1	108.1(2)	O1–N1–C3	110.4(12)
O1–N1–C2	109.9(2)	C1–N1–C2	110.0(12)
O1–N1–C3	104.6(2)	C1–N1–C3	114.4(12)
C1–N1–C2	112.1(2)	C2–N1–C3	111.9(12)
C1–N1–C3	110.7(2)	O2–N2–C4	108.8(12)
C2–N1–C3	111.2(2)	O2–N2–C5	106.9(13)
O2–N2–C4	107.5(3)	O2–N2–C6	104.0(12)
O2–N2–C5	106.1(3)	C4–N2–C5	115.6(12)
O2–N2–C6	107.7(3)	C4–N2–C6	107.4(12)
C4–N2–C5	111.6(3)	C5–N2–C6	113.5(12)
C4–N2–C6	111.4(3)		
C5–N2–C6	112.3(3)		

Symmetry codes: #1, (*x*, 1/2-*y*, *z*)

Table S4. Calculated spontaneous strains for the *mmm*F2/*m* ferroelastic species.

Compounds	β / °	ε_{13}	ε_{22}	ε_{33}	ε_{ss}	Ref
$(C_5N_2H_{16})_2[SbBr_5]$	116.79	-0.2223	-0.0006	-0.1195	0.355	S5
$(C_3H_5NH_3)_2[CdCl_4]$	108.54	-0.1608	-0.0386	-0.0412	0.239	S6
$(C_4H_9N)_2[PbBr_4]$	105.32	-0.1310	0.0034	-0.0433	0.191	S7
$(C_7H_{13}NH_3)_2[SnI_4]$	100.81	-0.0932	-0.0039	-0.0237	0.134	S8
1	100.24	-0.0875	0.0024	-0.0317	0.129	This work
$(Me_4P)_4[Mn(SCN)_6]$	97.70	-0.0648	0.0017	-0.0425	0.102	S9
$(Me_3NCH_2Br)_2[CoBr_4]$	93.44	-0.0308	0.0360	0.0247	0.068	S10
$(Me_3NCH_2Br)_2[ZnBr_4]$	93.54	-0.0305	-0.0021	-0.0151	0.048	S11
(N‑Methylpyrrolidinium)$[MnCl_3]$	93.19	-0.0279	-0.0033	0.0025	0.045	S12
$(Me_3NCH_2Cl)_2[ZnCl_4]$	93.35	-0.0289	-0.0137	-0.0113	0.045	S13
N-methylcyclohexylamine picrate	93.47	-0.0302	0.0034	-0.0040	0.044	S14
$(C_5H_{12}N)[CdCl_3]$	92.30	-0.0196	0.0139	-0.0249	0.040	S15
$(F\text{-}TEDA)(BF_4)_2$	91.99	-0.0170	-0.0088	-0.0206	0.033	S16
$(C_6H_{14}N)[PbI_3]$	92.09	-0.0181	-0.0177	-0.0059	0.032	S17
$(NMe_4)_2[HgCl_4]$	89.64	0.0031	-0.0100	-0.0238	0.027	S18
$[C_7H_7NOF_3(18\text{-crown-}6)]PF_6$	90.01	-0.0001	-0.0032	-0.0035	0.016	S19
$(C_3H_4NS)[CdBr_3]$	90.53	-0.0046	0.0012	-0.0003	0.009	S20
$(C_3H_4NS)[CdCl_3]$	90.23	-0.0020	0.0005	-0.0018	0.008	S21

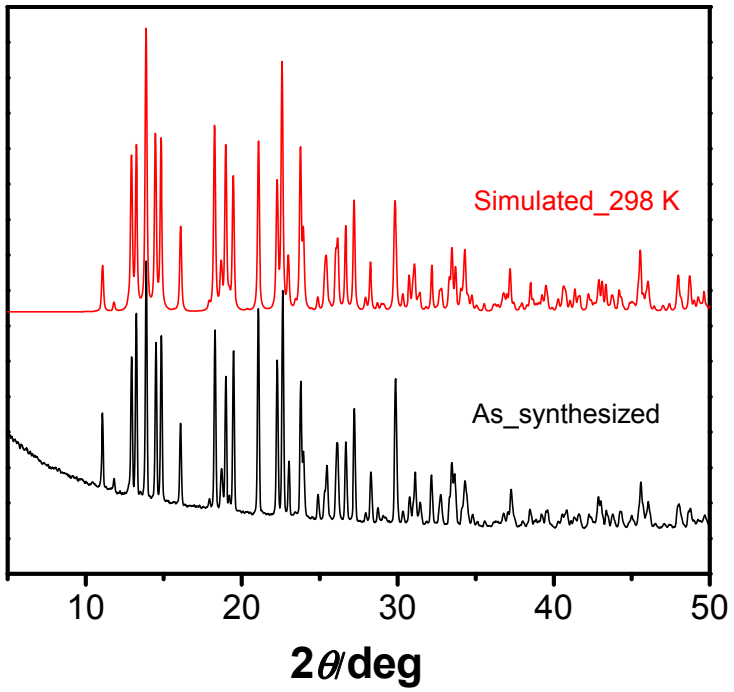

Figure S1. The PXRD patterns confirmed the phase purity of the as-synthesized sample **1**.

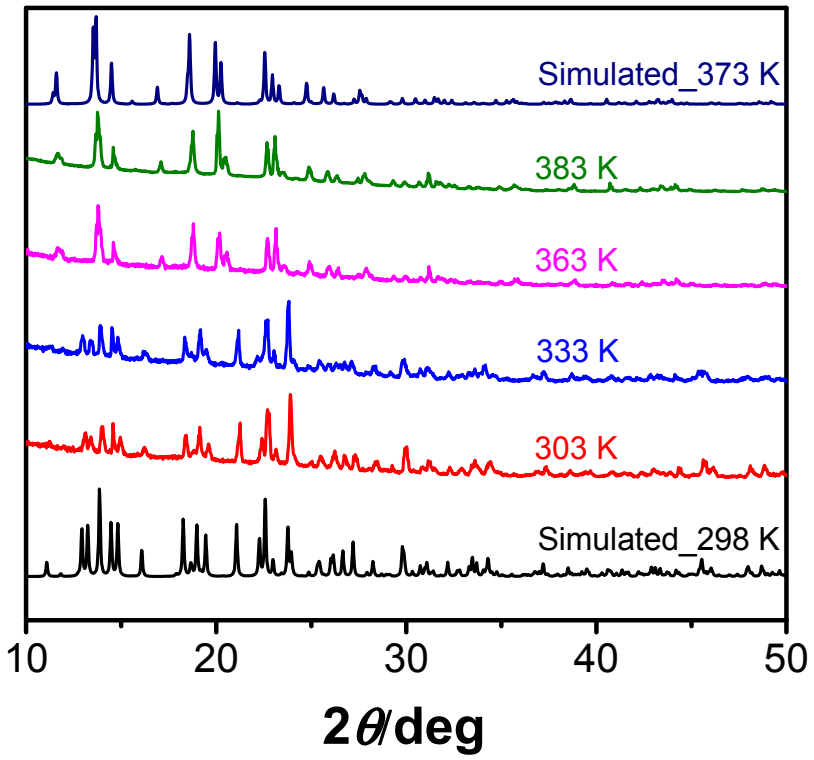

Figure S2. The variable-temperature powder X-ray diffraction patterns of **1**.

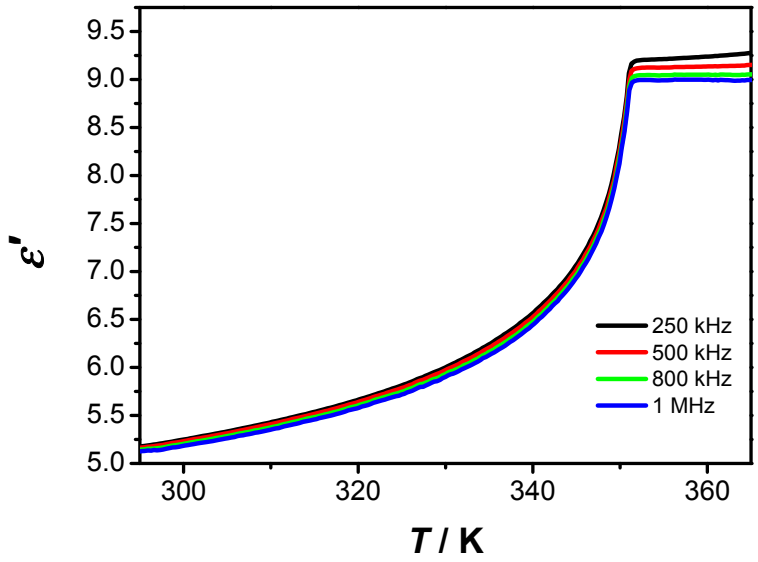

Figure S3. Temperature dependence of ε' of **1** measured on the powder sample at 250-1000 kHz.

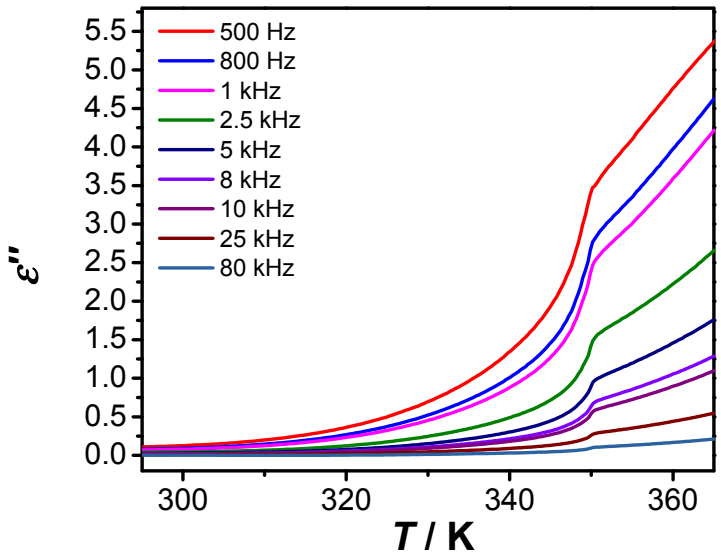

Figure S4. Temperature dependence of ε'' of **1** measured on the powder sample at 0.5-80 kHz.

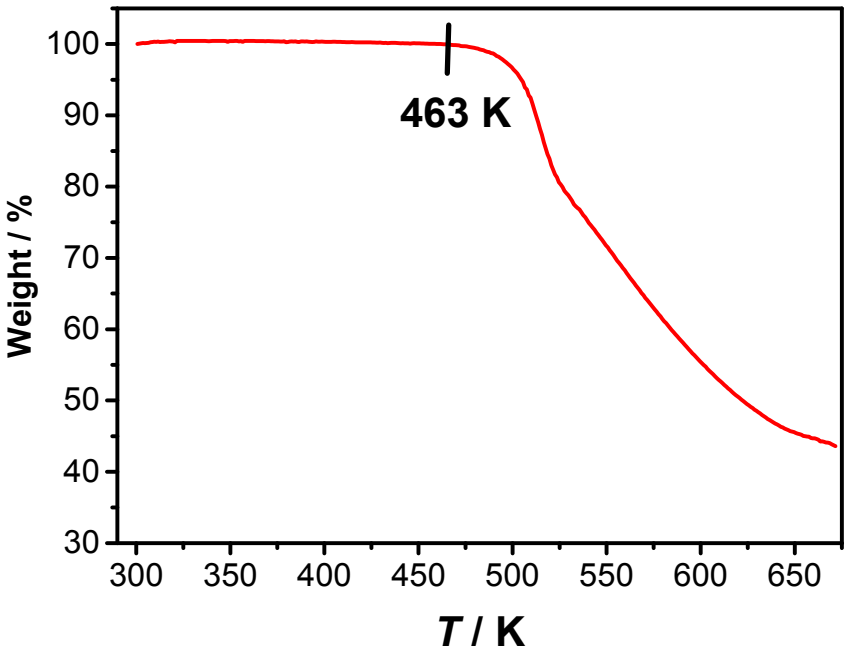

Figure S5. TG profiles of **1**.

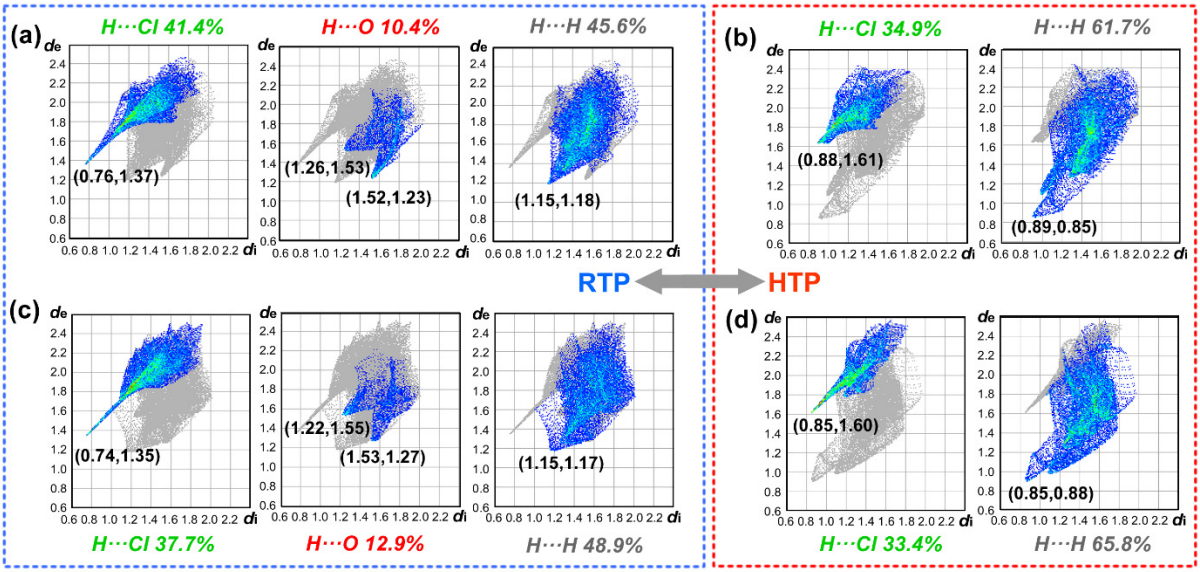

Figure S6. Decomposed fingerprint plots for **1** resolved into H···Cl, H···O and H···H contacts. Upper for Me_3NOH^+ with O1 atom and the bottom for Me_3NOH^+ with O2 atom.

Reference

S1. O. V. Dolomanov, L. J. Bourhis, R. J. Gildea, J. A. K. Howard and H. Puschmann, *J. Appl. Crystallogr.*, 2009, **42**, 339-341.

S2. K. Aizu, *J. Phys. Soc. Jpn.*, 1969, **27**, 387-396.

S3. K. Aizu, *J. Phys. Soc. Jpn.*, 1970, **28**, 706-716.

S4. J. Sapriel, *Phys. Rev. B*, 1975, **12**, 5128.

S5. C.-Y. Mao, W.-Q. Liao, Z.-X. Wang, Z. Zafar, P.-F. Li, X.-H. Lv and D.-W. Fu, *Inorg. Chem.*, 2016, **55**, 7661-7666.

S6. S. Han, X. Liu, J. Zhang, C. Ji, Z. Wu, K. Tao, Y. Wang, Z. Sun and J. Luo, *J. Mater. Chem. C*, 2018, **6**, 10327-10331.

S7. Z.-X. Wang, W.-Q. Liao, H.-Y. Ye and Y. Zhang, *Dalton Trans.*, 2015, **44**, 20406-20412.

S8. X.-N. Li, P.-F. Li, Z.-X. Wang, P.-P. Shi, Y.-Y. Tang and H.-Y. Ye, *Polyhedron*, 2017, **129**, 92-96.

S9. Q. Li, P.-P. Shi, Q. Ye, H.-T. Wang, D.-H. Wu, H.-Y. Ye, D.-W. Fu and Y. Zhang, *Inorg. Chem.*, 2015, **54**, 10642-10647.

S10. X.-N. Hua, C.-R. Huang, J.-X. Gao, Y. Lu, X.-G. Chen and W.-Q. Liao, *Dalton Trans.*, 2018, **47**, 6218-6224.

S11. J.-X. Gao, X.-N. Hua, P.-F. Li, X.-G. Chen and W.-Q. Liao, *J. Phys. Chem. C*, 2018, **122**, 23111-23116.

S12. X.-F. Sun, P.-F. Li, W.-Q. Liao, Z. Wang, J. Gao, H.-Y. Ye and Y. Zhang, *Inorg. Chem.*, 2017, **56**, 12193-12198.

S13. W.-Q. Liao, J.-X. Gao, X.-N. Hua, X.-G. Chen and Y. Lu, *J. Mater. Chem. C*, 2017, **5**, 11873-11878.

S14. K. Tao, Z. Wu, S. Han, J. Zhang, C. Ji, Y. Wang, W. Zhang, J. Luo and Z. Sun, *J. Mater. Chem. C*, 2018, **6**, 4150-4155.

S15. A. Zeb, Z. Sun, T. Khan, M. A. Asghar, Z. Wu, L. Li, C. Ji and J. Luo, *Inorg. Chem. Front.*, 2017, **4**, 1485-1492.

S16. Y.-W. Zhang, P.-P. Shi, W.-Y. Zhang, Q. Ye and D.-W. Fu, *Inorg. Chem.*, 2018, **57**, 10153-10159.

S17. A. Zeb, Z. Sun, A. Khan, S. Zhang, T. Khan, M. A. Asghar and J. Luo, *Inorg. Chem. Front.*, 2018, **5**, 897-902.

S18. M. Amami, S. van Smaalen, L. Palatinus, A. Ben Salah, X. Helluy and A. Sebald, *Z. Kristallogr. Cryst. Mater.*, 2002, **217**, 532.

S19. P.-F. Li, W.-Q. Liao, Q.-Q. Zhou, H.-Y. Ye and Y. Zhang, *Inorg. Chem. Commun.*, 2015, **61**, 77-81.

S20. W.-Q. Liao, H.-Y. Ye, Y. Zhang and R.-G. Xiong, *Dalton Trans.*, 2015, **44**, 10614-10620.

S21. G.-Q. Mei and W.-Q. Liao, *J. Mater. Chem. C*, 2015, **3**, 8535-8541.